

Neutral heavy lepton production at next high energy e^+e^- linear colliders

F.M.L. Almeida Jr.^{*}, Y. A. Coutinho[†],
J. A. Martins Simões[‡], M.A.B. do Vale[§]
Instituto de Física

Universidade Federal do Rio de Janeiro, RJ, Brazil

The discovery potential for detecting new heavy Majorana and Dirac neutrinos at some recently proposed high energy e^+e^- colliders is discussed. These new particles are suggested by grand unified theories and superstring-inspired models. For these models the production of a single heavy neutrino is shown to be more relevant than pair production when comparing cross sections and neutrino mass ranges. The process $e^+e^- \rightarrow \nu e^\pm W^\mp$ is calculated including on-shell and off-shell heavy neutrino effects. We present a detailed study of cross sections and distributions that shows a clear separation between the signal and standard model contributions, even after including hadronization effects.

PACS: 12.60.-i, 13.85.-t, 14.60.-z

The recent Super-Kamiokande results [1] provided a strong evidence for neutrino oscillations and non zero neutrino masses. This has motivated many theoretical models that imply new heavy neutrino states. These new particles are present in several grand unified extensions of the standard model such as $SO(10)$ or E_6 . Many other new states are present in these models but neutrinos are expected to play a fundamental role in any consistent extended model. This comes mainly from the possibility that light neutrino masses can be connected to the Fermi and grand unified scales through $m_\nu = v_{Fermi}^2/v_{GUT}$. This relation can be obtained from the "see-saw" mechanism with new heavy neutrino states. A fundamental point to be experimentally clarified is the Dirac or Majorana nature of neutrinos.

The new heavy neutrino masses are experimentally bounded to be greater than 80-100 GeV [2,3] and the mixing with light neutrinos is expected to be small, even if there is some model dependence on these results. This means that these new neutral leptons could be detected only at the next generation of high energy colliders NLC at SLAC and TESLA at DESY. In this paper we turn our attention to these new possible lepton colliders [4]. New linear e^+e^- high energy colliders have been proposed, with center of mass energy from 500 GeV up to a few TeV. More recently $\mu^+\mu^-$ and e^-e^- options were also proposed, as well as the electron-muon colliders.

Some time ago it was noticed [5,6] that for some models the single heavy lepton production in $e^+e^- \rightarrow \nu N$ is higher than pair production $e^+e^- \rightarrow NN$. Two main factors contribute for this difference. The first one is the

mixing angle ($s_i \equiv \sin \theta_{mix}$) single power in the light-to-heavy neutrino vertex, contrary to the double mixing angle power in the heavy-to-heavy neutrino vertex. The second factor is phase space suppression. If we suppose that all mixing angles are of the same order, then we have in Table I the vertices for heavy neutrino interactions in three different models [5] for new heavy neutrino states: vector singlet (VSM), vector doublet (VDM) and fermion-mirror-fermion models (FMFM). We call attention to the suppression factor for the ZNN vertex in the vector singlet model, which is not present for the other models. Throughout this paper we will suppose that mixing angles for heavy-to-light neutrinos and new heavy neutrino masses are independent parameters. In the naive see-saw model, the mixing between light and heavy neutrinos is given by $\theta \simeq \frac{m_\nu}{m_N}$. However, there are many theoretical models which decouple the mixing from the mass relation [7]. The mechanism is very simple. In the general mass matrix including Dirac and Majorana fields one imposes some internal symmetry that makes the matrix singular. Then the mixing parameter has an arbitrary value, bounded only by its phenomenological consequences.

Recently we have investigated this possibility for a single heavy Majorana production in hadron-hadron colliders [8]. It was shown that this mechanism is more important than pair production and that like-sign dileptons can give a clear signature for this process, even after hadronization. The mixing of the presently known fermions and possible new heavy states is known to be small, of the order of $\sin^2 \theta_{mix} = 10^{-2} - 10^{-3}$. This comes

^{*}E-mail: marroqui@if.ufrj.br

[†]E-mail: yara@if.ufrj.br

[‡]E-mail: simoes@if.ufrj.br

[§]E-mail: aline@if.ufrj.br

from low energy phenomenology and the high precision measurements of the Z properties at LEP/SLC. A recent estimate [9] gives $\sin^2 \theta_{mix} < 0.0052$ with 95% C.L. This limit value is used throughout this paper for all curves and distributions.

In this paper we present the complete first order treatment of single heavy neutral lepton production in electron-positron high energy colliders, including finite width effects. The full first order standard model background is also considered. We have studied the general process $e^+e^- \rightarrow \nu_\ell \ell W$ where ℓ is a charged lepton and ν_ℓ is a light neutrino or antineutrino. For the signal we can have the diagram contributions as shown in Fig. 1. Some earlier studies [5,6,10] were done in the heavy neutrino on-shell approximation which includes diagrams (a) and (d) in Fig. 1. It is known that for energies well above the Z mass the s -channel is suppressed and t -channel is dominant for N exchange. As we are interested in the study of distributions and experimental cuts, we have taken into account all the diagrams shown in Fig. 1 for the process $2 \rightarrow 3$. We can have lepton number conservation or violation, depending on the Dirac or Majorana nature of neutrinos, respectively. In this paper we consider three different heavy neutrinos, one for each family. For Dirac heavy neutrinos we have lepton number conservation. Majorana neutrinos carry no internal quantum numbers and we are then supposing that all the vertices NeW ; $N\mu W$ and $N\tau W$ have the same strength. In this case we are considering only the lighter Majorana state. At the Fermi scale these new states are expected to behave as $SU_L(2) \otimes U_Y(1)$ basic representations.

We can resume these interactions in the neutral and charged current lagrangians:

$$\mathcal{L}_{nc} = -\frac{g}{2c_W} Z_\mu \bar{\psi}_i \gamma^\mu (g_V^{ij} - g_A^{ij} \gamma_5) \psi_j. \quad (1)$$

and

$$\mathcal{L}_{cc} = -\frac{g}{2\sqrt{2}} W_\mu \bar{\psi}_i \gamma^\mu (a^{ij} - b^{ij} \gamma_5) \psi_j. \quad (2)$$

where i, j are the appropriate combination of e, ν, N with “ N ” the new neutral lepton. The light neutrino couplings to the neutral Z are given by $g_{V,A} = g_{V,A}^{SM} - \sin^2 \theta_{mix}/2$.

The decay modes for these leptons, in the Dirac case, are $N_e \rightarrow e^- W^+$ and $N_e \rightarrow \nu_e Z$. For Majorana neutrinos [8] we must include both signatures $N \rightarrow \ell^\mp W^\pm$ and $N \rightarrow \nu_\ell (\bar{\nu}_\ell) Z$, with $\ell = e, \mu, \tau$.

In Fig. 2 we show the total cross sections for single $e^+e^- \rightarrow \nu N$ and pair heavy lepton production $e^+e^- \rightarrow NN$ at $\sqrt{s} = 500$ GeV. All curves are for on-shell heavy neutrinos. A single heavy Majorana has the higher cross section due to the sum over final neutrino and anti-neutrino production and to the sum over the three lepton families. The single heavy Dirac neutrino for the electron family dominates the associated

muon (and tau) family production since in the first case we have s and t channel exchanges, whereas in the last cases we have only s channel contribution. Similar arguments apply to the pair production of heavy neutrinos. In the vector singlet model we have a strong suppression factor from the ZNN vertex in the s channel. For the other models we also have an energy suppression in the amplitude from the Z propagator in the s channel and a $\sin^2 \theta_{mix}$ for the t channel. In all cases, pair production is kinematically bounded to masses up to $\sqrt{s}/2$ whereas single heavy neutrino production can reach masses up to \sqrt{s} . For center of mass energy of 1 TeV a similar pattern of heavy neutrino production is present. For the more specific sub-process $e^+e^- \rightarrow \nu e^+ W^-$ a careful distinction between Dirac and Majorana neutrinos must be done and the correct set of Feynman diagrams must be chosen from Fig. 1. An important point on the Dirac or Majorana nature of the new possible heavy neutrino comes from Fig. 2. For a heavy Dirac neutrino the electron final state is two orders of magnitude greater than the final state muon. For a Majorana heavy neutrino we expect an equal number of electrons and muons in the final state. Another point to be taken into account is the fact that the final state light neutrino is an experimentally undetected particle. So we must sum over all possible combinations whenever necessary. In all cases we have considered all contributions, with on-shell and off-shell single heavy neutrinos, as well as finite width effects, as recently investigated by Cvetic, Kim and Kim [11]. The standard model background contributes with 12 diagrams, as shown in Fig. 3. Both the signal and background were calculated using the high energy program CompHep [12].

Let us now turn our attention to the general characteristics of the process $e^+e^- \rightarrow \nu e^+ W^-$. In Figs. 4-12 we have done simple detector cuts $E_{lepton} > 5$ GeV and $-0.995 < \cos \theta_i < 0.995$, where θ_i is the angle between any final state particle and the initial electron. We define θ_{e^+} as the angle between the initial electron and the final state positron; θ_{W^-} as the angle between the initial electron and the final state W^- or hadrons and $\theta_{e^+ W^-}$ as the angle between the final positron and the final state W^- or hadrons, in the e^+e^- center of mass frame.

In Fig. 4 we show the total cross section for the signal and standard model background, which is typically 1-1.5 orders of magnitude greater than the signal. One of the main points of our work is to show that this relation will be inverted by appropriated cuts in the e^+W^- invariant mass distribution. In order to justify our cuts, let us first look at the following angular distributions. In Figs. 5 and 6 we display the final state positron angular distribution (relative to the initial electron) for $M_N = 100$ and $M_N = 400$ GeV in the Majorana and Dirac cases, as well as the standard model contribution. We have taken these two mass values, one below and the other above the pair production mass limit. We notice that for smaller masses, around 100 GeV, the Majorana and Dirac cases are different, but for higher masses this difference disap-

pears. A similar situation is seen in Figs. 7 and 8 for the W angular distribution. The intermediate masses of heavy neutrinos can be easily inferred from Figs. 5-8.

In Fig. 9 we show the angular distribution between the final e^+ and W^- in the e^+e^- center of mass frame, for a heavy Majorana neutrino. The signal presents a clear kinematical bound from the Lorentz boost along the heavy neutrino direction. In the Dirac neutrino case we have a similar shape, above the Majorana curves.

In order to have a more realistic estimate of the signal-to-background separation we have performed the W^- hadronization using the Pythia program [13], for the signal and the standard model background. Another possible background source is the process $e^+e^- \rightarrow e^+e^-Z$ where the final state electron escapes detection. With the hadron jets peaked around the Z mass, we have verified that this channel has a small contribution to the dominant background.

The invariant visible mass ($e^+ + \text{hadrons}$) versus missing (neutrinos) energy correlations are shown in Figs. 10-12, in arbitrary units. In Figs. 10-11-12, labeled “a” we have applied the following general detector cuts: $-0.95 < \cos\theta_{e^+} < 0.995$ and $-0.995 < \cos\theta_{W^-} < 0.95$. Here we have a very clear limited kinematical region coming from energy-momentum conservation. The signal is already present in these figures. The angular distributions in Figs. 5-9 suggests that the signal-to-background can be increased by applying more restrictive angular cuts. The results are shown in Figs. 10b.; 11b.; 12b. For a heavy neutrino mass of 100 GeV we have done $-0.5 < \cos\theta_{e^+W^-} < 0.995$ and the result is shown in Fig. 11a. For a mass $M_N = 200$ GeV the results are shown in Fig. 11b., with angular cuts $-0.9 < \cos\theta_{e^+} < 0.995$; $-0.5 < \cos\theta_{e^+W^-} < 0.5$; $-0.95 < \cos\theta_{W^-} < 0.9$. For a heavy neutrino mass of 400 GeV we have Fig. 12b., with angular cuts $-0.5 < \cos\theta_{e^+} < 0.995$; $-0.95 < \cos\theta_{W^-} < 0.5$; $-0.95 < \cos\theta_{e^+W^-} < -0.7$. These more restrictive angular cuts show quite clearly that the ratio signal/background can be improved. For center of mass energies of 1 TeV we found analogous conclusions.

In conclusion, the present work shows that e^+e^- colliders can test the existence of heavy Dirac and Majorana neutrino masses up to \sqrt{s} in the νe^\pm hadrons channel. For higher center of mass energies the conclusions are similar to the case of a $\sqrt{s} = 500$ GeV presented in detail in this paper, since the process is dominated by t channel exchange. For $\mu^+\mu^-$ colliders we have the same situation, if we replace the final e^+ by a μ^+ . Single heavy neutrino production bellow and above pair mass threshold can be clearly separated from the standard model background, even after hadronization and detector cuts. Angular cuts on the final state particle distributions can be applied unambiguously, in order to increase the signal-to-background ratio. As our estimate for the signal cross section uses the upper bound for $\sin^2\theta_{mix}$, an eventually negative experimental search can be converted into new more restrictive light-to-heavy neutrino mixing bound.

Acknowledgments: This work was partially supported by the following Brazilian agencies: CNPq, FUJB, FAPERJ and FINEP.

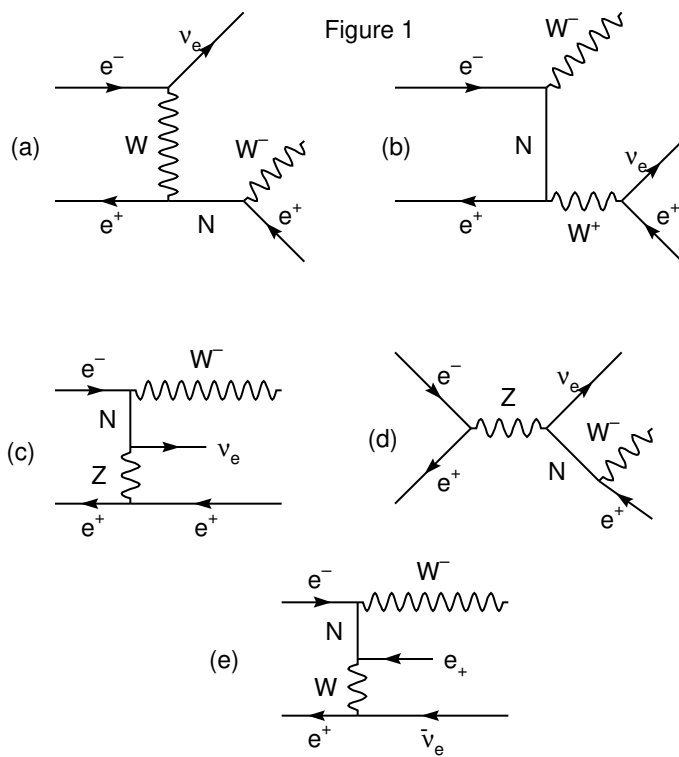
-
- [1] A. Mann, hep-ex/9912007.
 - [2] K. Zuber, Phys. Rep. **305** (1998) 295.
 - [3] D.E. Groom et al, Eur. Phys. Jour. **C15** (2000) 1.
 - [4] The development of future linear electron positron colliders: for particle physics and for research using free electron lasers. Proceedings, Workshop, Lund, Sweden, September 23-25, 1999. By G. Jarlskog, (ed.), U. Mjornmark, (ed.), T. Sjostrand, (ed.) (Lund U.). 1999. 331pp. Geneva, Switzerland: CERN (1999) 331 p.
 - [5] F.M.L. Almeida Jr., J.H. Lopes, J.A. Martins Simões and C.M. Porto Phys. Rev. D**44** (1991) 2836 ; F.M.L. Almeida Jr., J.H. Lopes, J.A. Martins Simões, P. P. Queiroz Filho and A. J. Ramalho Phys. Rev. D**51** (1994) 5990.
 - [6] A. Djouadi Z. Phys. C**63** (1994)317; G. Azuelos, A. Djouadi Z. Phys. C**63** (1994)327.
 - [7] C. Jarlskog, Phys. Lett. B**241**,579 (1990); D. Tommasini, G. Barenboim, J. Bernabéu and C. Jarlskog, Nuc. Phys. B**444**,451 (1994); W. Buchmüller, C. Creub and P. Minkowski, Phys. Lett. B**267**,355(1991).
 - [8] F.M.L. Almeida Jr., Y.A. Coutinho, J.A. Martins Simões, P.P. Queiroz Filho and C.M.Porto, Phys. Lett. B**400** (1997) 331.
 - [9] F.M.L. Almeida Jr., Y.A. Coutinho, J.A. Martins Simões, M.A.B. do Vale, Phys. Rev. D**62** (2000) 075004.
 - [10] A. Djouadi, J. Ng and T.G. Rizzo in: Electroweak Symmetry Breaking and Beyond the Standard Model. Ed.T. Barklow, S. Dawson, H.E. Haber and S.Siegrist, World Scientific, Singapore. hep-ph 9504210; P.Langacker, M. Luo and A.K. Mann, Rev. Mod. Phys. **64** (1992) 87.
 - [11] G. Cvetič, C.S. Kim and C.W. Kim Phys. Rev. Lett.**82** (1999)4761.
 - [12] A. Pukhov, E. Boss, M. Dubinin, V. Edneral, V. Ilyin, D. Kovalenko, A. Krykov, V. Savrin, S. Shichanin and A. Semenov, "CompHEP"- a package for evaluation of Feynman diagrams and integration over multi-particle phase space. Preprint INP MSU 98-41/542, hep-ph/9908288.
 - [13] T. Sjöstrand, Comp. Phys. Commun. **82**,74 (1994).

Figure Captions

1. Signal Feynman graphs for heavy Majorana (N) and Dirac (N_e, N_μ) neutrino contribution to $e^+e^- \rightarrow \nu e^+ W^-$.
2. Single and pair production of on-shell heavy Dirac (VSM, VDM and FMFM) and Majorana neutrinos at $\sqrt{s} = 500$ GeV for e^+e^- colliders ($\sin^2 \theta_{mix} = 0.0052$).
3. Standard model background contribution to $e^+e^- \rightarrow \nu e^+ W^-$.
4. Signal and background (standard model) contributions to $e^+e^- \rightarrow \nu e^+ W^-$ at $\sqrt{s} = 500$ GeV.
5. Final positron angular distribution relative to the initial electron for heavy Majorana neutrinos with $M_N = 100$ GeV and $M_N = 400$ GeV.
6. Final positron angular distribution relative to the initial electron for heavy Dirac neutrinos with $M_N = 100$ and $M_N = 400$ GeV.
7. W^- angular distribution relative to the initial electron for heavy Majorana neutrinos with $M_N = 100$ GeV and $M_N = 400$ GeV.
8. W^- angular distribution relative to the initial electron for heavy Dirac neutrinos with $M_N = 100$ GeV and $M_N = 400$ GeV.
9. Angular distribution between final positron and W^- for heavy Majorana neutrinos with $M_N = 100$ GeV, $M_N = 200$ GeV and $M_N = 400$ GeV.
10. Invariant visible mass ($e^+ + \text{hadrons}$) versus missing (neutrino) energy correlation for background and signal for $M_N = 100$ GeV (in arbitrary units). Fig. 10a. was done with the general cuts and Fig. 10b. was done with the additional cuts as discussed in the text.
11. Same as figure 10 for $M_N = 200$ GeV.
12. Same as figure 10 for $M_N = 400$ GeV.

	VSM	VDM	FMFM
$W \rightarrow eN$	$a = s_i$ $b = s_i$	$a = s_i$ $b = -s_i$	$a = 0$ $b = 2s_i$
$Z \rightarrow \nu N$	$g_V = s_i/2$ $g_A = s_i/2$	$g_V = s_i/2$ $g_A = -s_i/2$	$g_V = 0$ $g_A = s_i$
$Z \rightarrow NN$	$g_V = s_i^2/2$ $g_A = s_i^2/2$	$g_V = 1$ $g_A = s_i^2/2$	$g_V = 1/2$ $g_A = -1/2$

TABLE I. Mixing angles for W and Z couplings with new neutral heavy leptons for three different models.



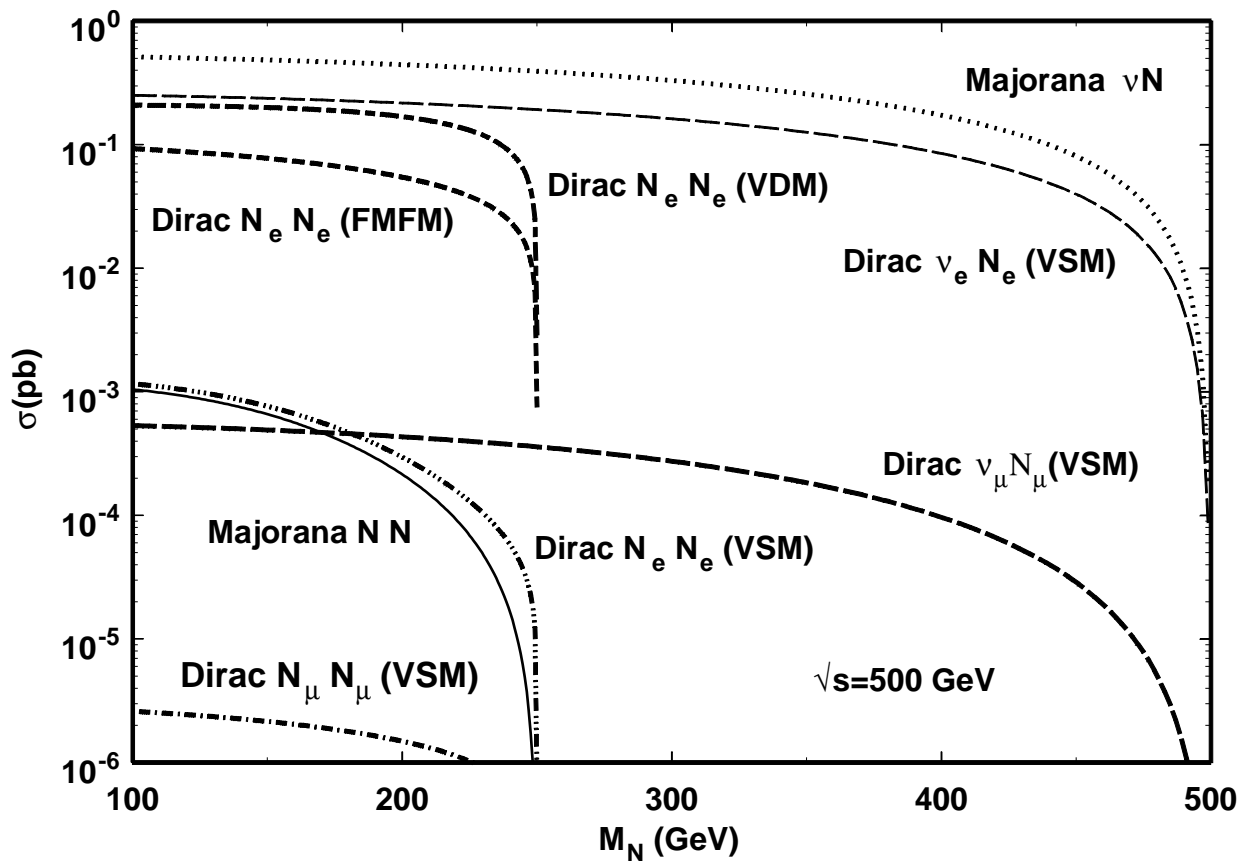


Figure 2

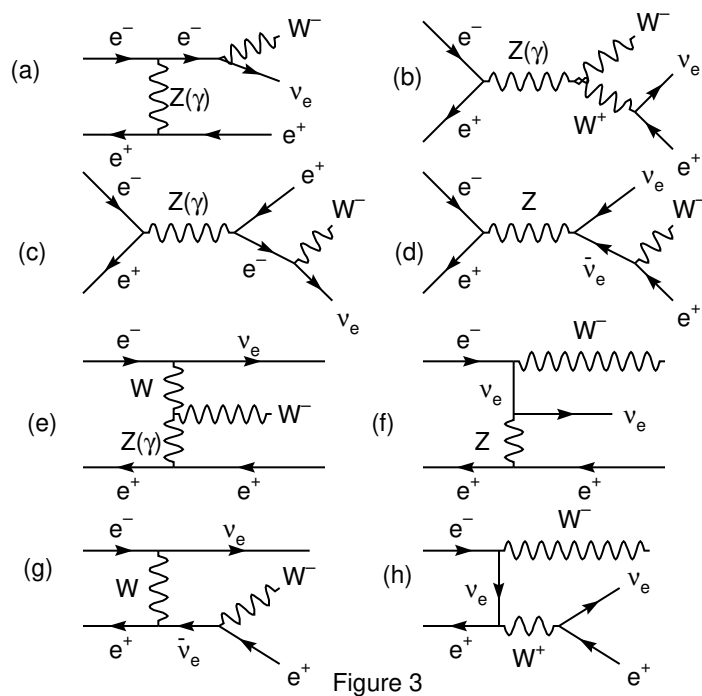


Figure 3

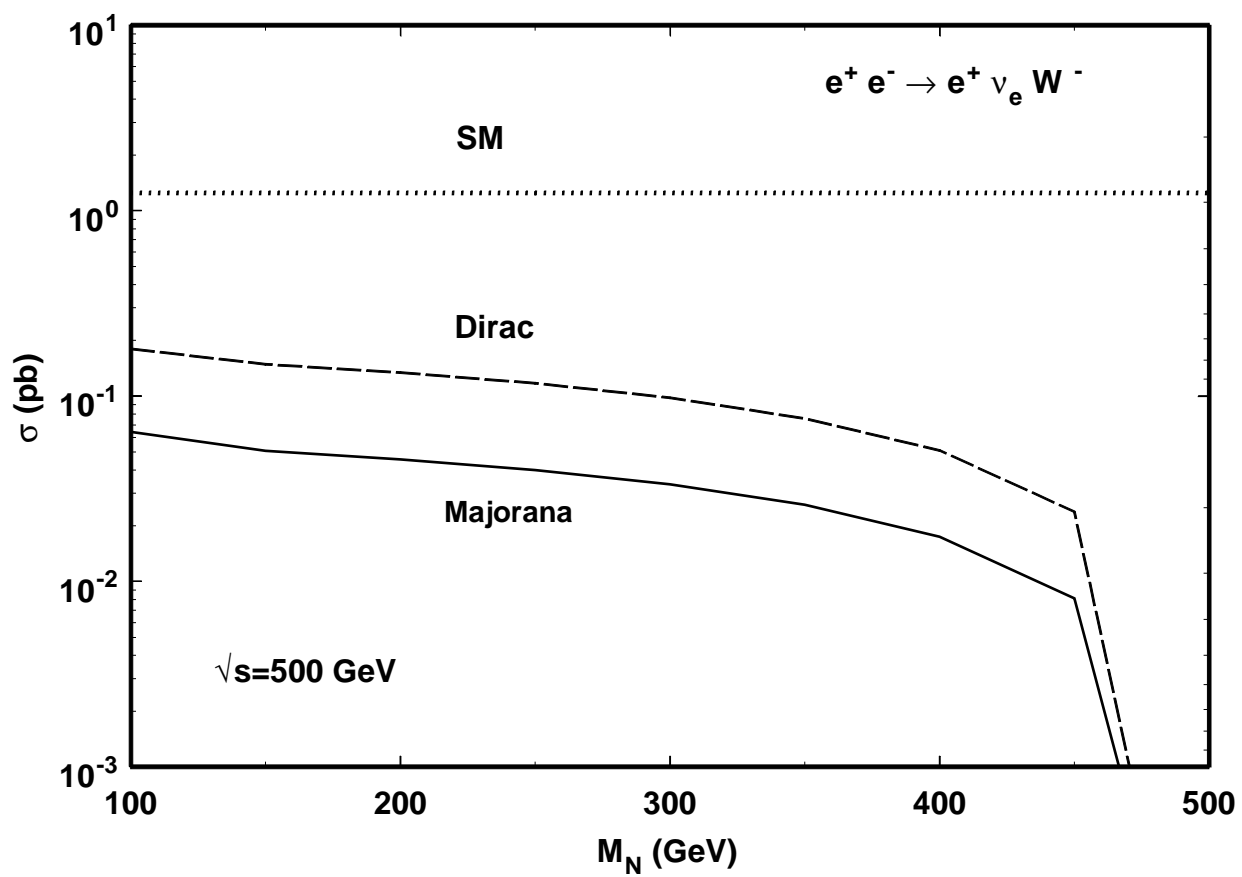


Figure 4

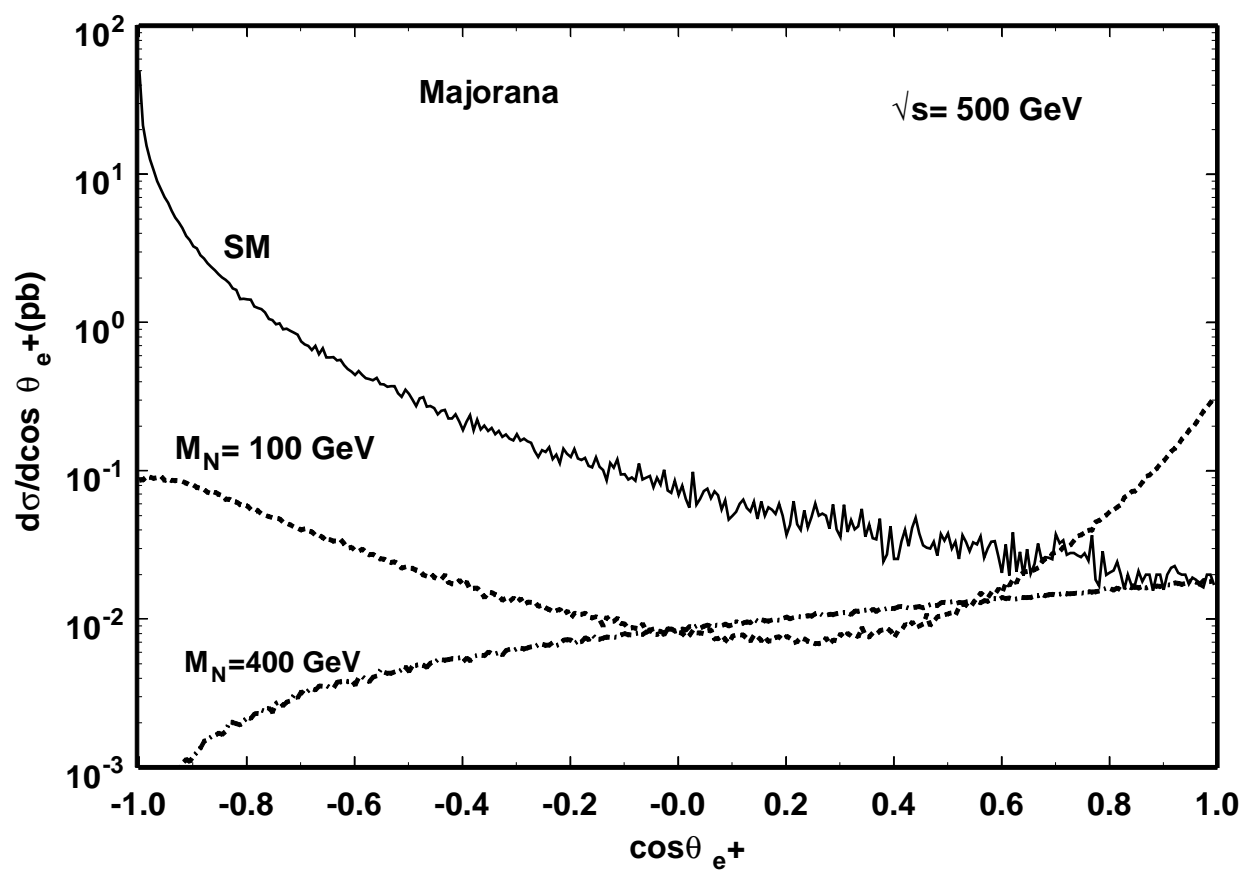


Figure 5

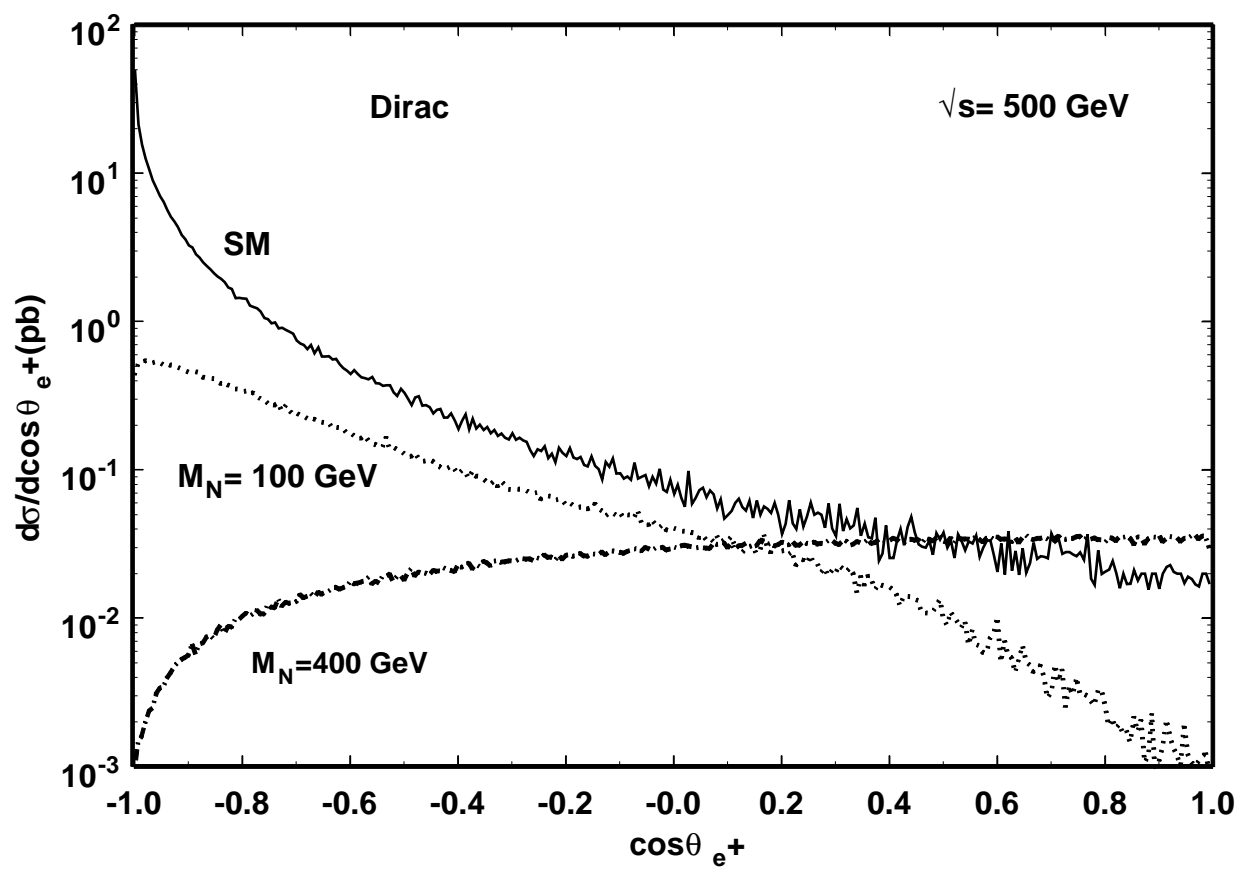


Figure 6

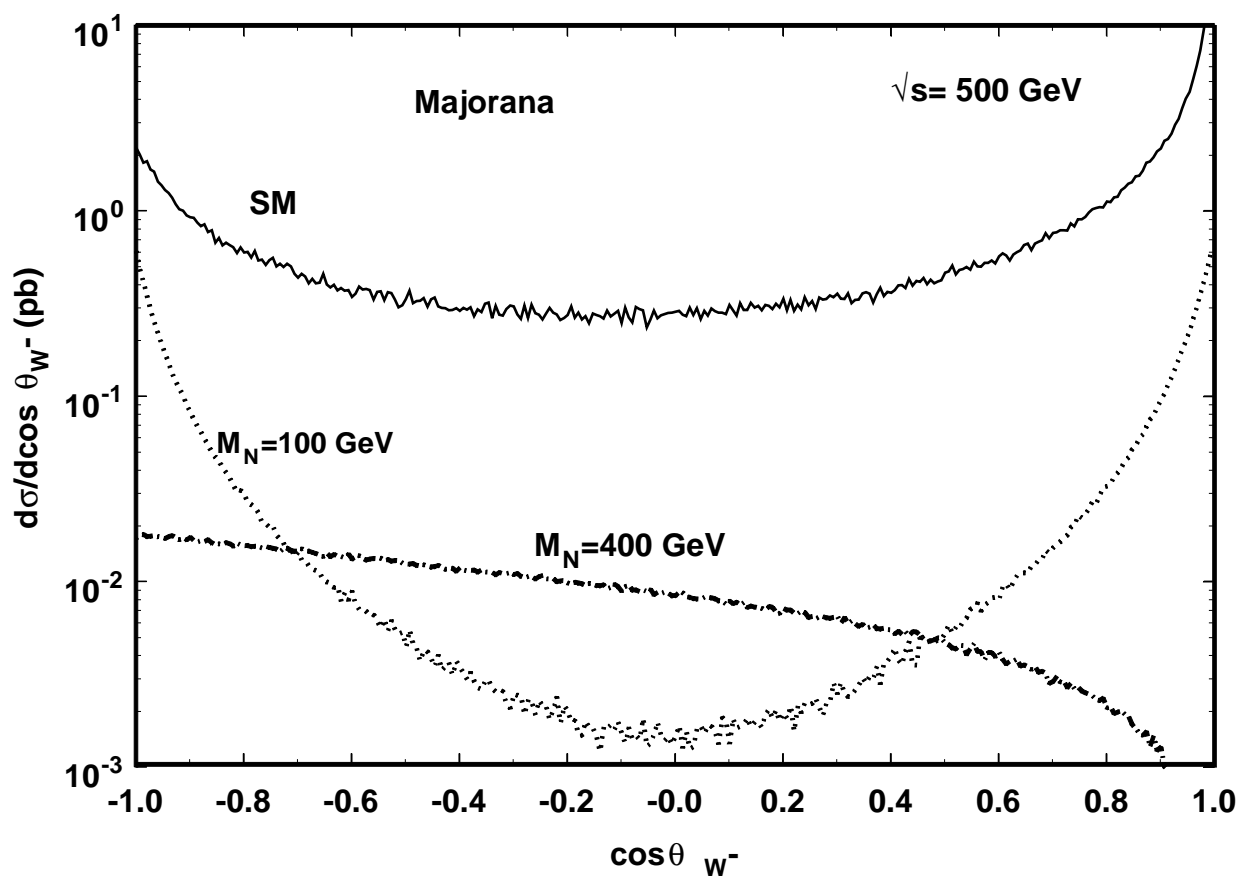


Figure 7

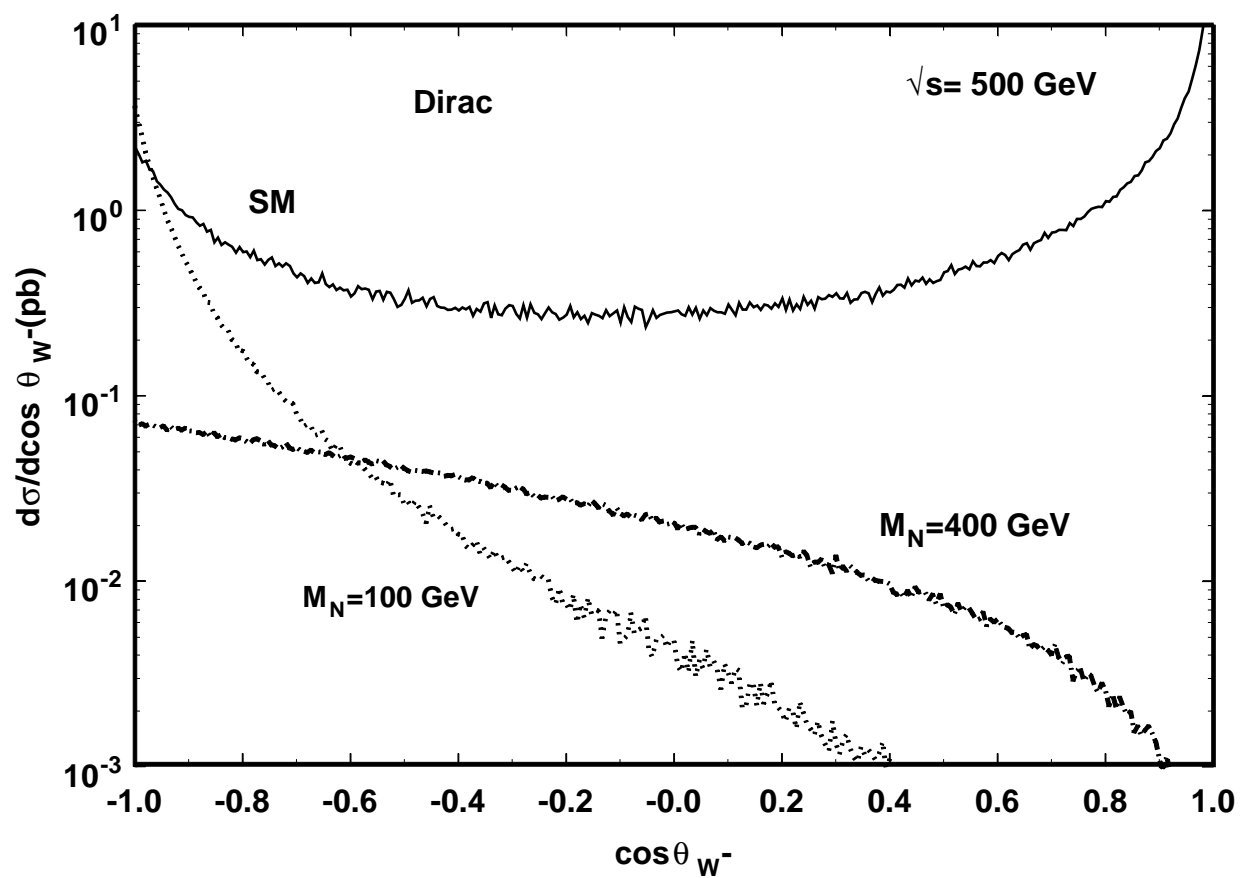


Figure 8

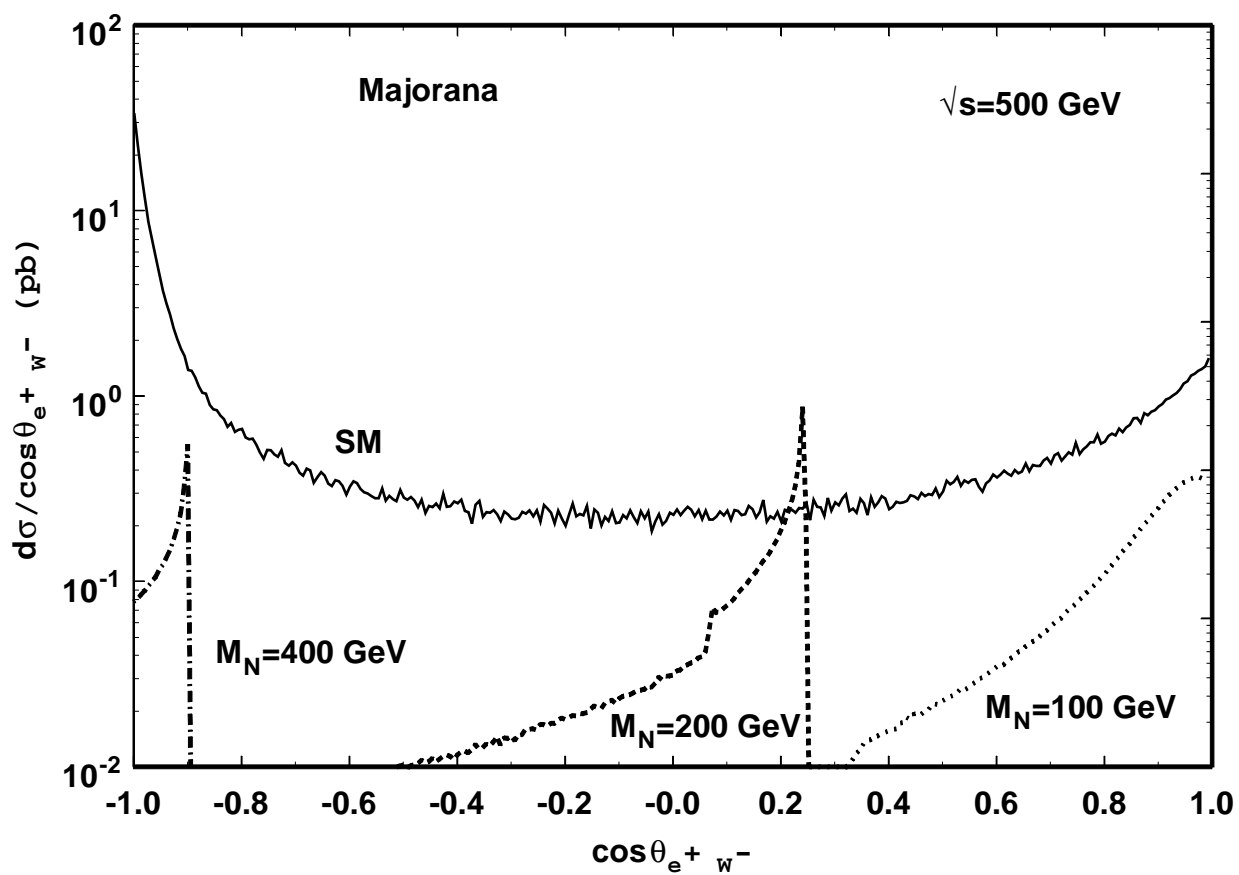


Figure 9

This figure "figure10a.jpg" is available in "jpg" format from:

<http://arxiv.org/ps/hep-ph/0008201v2>

This figure "figure10b.jpg" is available in "jpg" format from:

<http://arxiv.org/ps/hep-ph/0008201v2>

This figure "figure11a.jpg" is available in "jpg" format from:

<http://arxiv.org/ps/hep-ph/0008201v2>

This figure "figure11b.jpg" is available in "jpg" format from:

<http://arxiv.org/ps/hep-ph/0008201v2>

This figure "figure12a.jpg" is available in "jpg" format from:

<http://arxiv.org/ps/hep-ph/0008201v2>

This figure "figure12b.jpg" is available in "jpg" format from:

<http://arxiv.org/ps/hep-ph/0008201v2>